Responses of surface ozone air quality to anthropogenic nitrogen deposition in the Northern Hemisphere

Yuanhong Zhao[1], Lin Zhang[1], Amos P. K. Tai[2], Youfan Chen[1], Yuepeng Pan[3]

[1] Laboratory for Climate and Ocean-Atmosphere Sciences, Department of Atmospheric and Oceanic Sciences, School of Physics, Peking University, Beijing 100871, China

[2] Earth System Science Programme and Graduate Division of Earth and Atmospheric Sciences, Faculty of Science, The Chinese University of Hong Kong, Hong Kong SAR, China

[3] State Key Laboratory of Atmospheric Boundary Layer Physics and Atmospheric Chemistry (LAPC), Institute of Atmospheric Physics, Chinese Academy of Sciences, Beijing 100029, China

Correspondence to: Lin Zhang (zhanglg@pku.edu.cn)

Abstract. Human activities have substantially increased atmospheric deposition of reactive nitrogen to the Earth's surface, inducing unintentional effects on ecosystems with complex environmental and climate consequences. One consequence remaining unexplored is how surface air quality might respond to the enhanced nitrogen deposition through surface-atmosphere exchange. Here we combine a chemical transport model (GEOS-Chem) and a global land model (Community Land Model) to address this issue with a focus on ozone pollution in the Northern Hemisphere. We consider three processes that are important for surface ozone and can be perturbed by addition of atmospheric deposited nitrogen, namely, emissions of biogenic volatile organic compounds (VOCs), ozone dry deposition, and soil nitrogen oxide (NO_x) emissions. We find that present-day anthropogenic nitrogen deposition (65 Tg N a^{-1} to the land), through enhancing plant growth (represented as increases in vegetation leaf area index (LAI) in the model), could increase surface ozone from increased biogenic VOC emissions (e.g., a 6.6 Tg increase in isoprene emission), but could also decrease ozone due to higher ozone dry deposition

velocities (up to 0.02-0.04 cm s^{-1} increases). Meanwhile, deposited anthropogenic nitrogen to soil enhances soil NO_x emissions. The overall effect on summer mean surface ozone concentrations show general increases over the globe (up to 1.5-2.3 ppbv over the western US and South Asia), except for some regions with high anthropogenic NO_x emissions (0.5-1.0 ppbv decreases over the eastern US, Western Europe, and North China). We compare the surface ozone changes with those driven by the past 20-year climate and historical land use changes. We find that the impacts from anthropogenic nitrogen deposition can be comparable to the climate and land use driven surface ozone changes at regional scales, and partly offset the surface ozone reductions due to land use changes reported in previous studies. Our study emphasizes the complexity of biosphere-atmosphere interactions, which can have important implications for future air quality prediction.

1 Introduction

Reactive nitrogen, in the forms of reduced (NH_x) and oxidized nitrogen (NO_y), is an essential nutrient to the biosphere. Without human influence, reactive nitrogen is mainly fixed from inert nitrogen gas (N_2) through natural biological fixation, lightning, and wildfires (Galloway et al., 2004; Fowler et al., 2013). Human activities such as urbanization, industrialization, and agricultural development have led to the emissions of large amounts of reactive nitrogen in the forms of nitrogen oxides (NO_x = NO + NO_2) and ammonia (NH_3) since the preindustrial period. Their removal via atmospheric deposition has increased by more than a factor of three from the preindustrial era to the early 2000s, and become an important source of reactive nitrogen to terrestrial and oceanic ecosystems (Galloway et al., 2004; Liu et al., 2013; Zhao et al., 2017).

Assessing the consequences of atmospheric nitrogen deposition requires a deep understanding of the interactions and feedbacks within different components of the Earth system including the biosphere and the atmosphere. There is evidence that enhanced atmospheric nitrogen deposition has led to negative

effects such as soil acidification (Stevens et al., 2009; Lu et al., 2014), eutrophication (Rodríguez et al., 2006), and loss of biomass diversity (Baron et al., 2014). Atmospheric nitrogen deposition has also been shown to increase carbon storage in terrestrial and oceanic ecosystems, but the resulting climate benefits can be largely offset by increased emissions of nitrous oxide (N_2O), a major greenhouse gas, as a byproduct of enhanced microbial nitrification and denitrification in soils (Duce et al., 2008; Zaehle et al., 2011; Bala et al., 2013). Previous studies mainly focused on the land-atmosphere exchange of long-lived greenhouse gases including CO_2, N_2O, and CH_4 (Liu et al., 2009; Zaehle et al., 2011) and their effects on climate. Very few studies have explored how ecosystem-mediated feedbacks through atmospheric chemistry influence air quality. Here we will present such a study that investigates how human-induced atmospheric nitrogen deposition may affect atmospheric composition and air quality via modifying ecosystem structure in terms of foliage density, with a focus on surface ozone pollution.

Near-surface ozone is a harmful air pollutant that results in detrimental effects on human health and vegetation (Bates, 2005; Jerrett et al., 2009; Avnery et al., 2011). It is mainly formed in the troposphere by photochemical oxidation of carbon monoxide (CO) and VOCs in the presence of NO_x. Tropospheric ozone burden has more than doubled since preindustrial times, mainly driven by rising anthropogenic emissions of ozone precursors (NO_x, CO, and VOCs) and the recent equatorward shift of emission patterns (Young et al., 2013; Zhang et al., 2016). Ozone impact on plant growth is mainly affected through its stomatal uptake, and has been shown to severely damage forest, grassland and agricultural productivity (Ainsworth et al., 2012). Ozone damage impedes various foliage physiological functions including photosynthesis and stomatal conductance, with ramifications not only for ecosystem health but also for climate (Fowler et al., 2009; Matyssek et al., 2010; Yue et al., 2014; 2016; Sadiq et al., 2017). Major crops such as wheat, maize, rice, and soybean are also sensitive to surface ozone pollution, leading to concerns for global food security (Mills et al., 2007). Recent studies estimated that about 79-121 Tg of crop production was reduced due to ozone pollution in year 2000 alone (Avnery et

al., 2011), and future ozone damage on crops would lead to a 3.6% loss in total crop production under the Intergovernmental Panel on Climate Change (IPCC) RCP8.5 emission scenario (Tai et al., 2014).

The terrestrial biosphere can in turn affect surface ozone levels through surface-atmosphere exchange processes including biogenic VOC emissions, soil NO_x emissions, as well as ozone dry deposition loss (Heald and Geddes, 2016). A number of studies have investigated how surface air quality may respond to perturbations of these processes driven by historical land use change (Fu and Tai, 2015; Val Martin et al., 2015; Fu et al., 2016; Heald and Geddes, 2016) and climate change (Fu and Tai, 2015; Fu et al., 2016). Atmospheric nitrogen deposition, by enhancing plant growth and soil mineral nitrogen content, is thus expected to modulate the production and loss of surface ozone. In this study, we build an asynchronously coupled modeling system using the GEOS-Chem global atmospheric chemistry model and the Community Land Model (CLM) to quantify the responses of surface ozone air quality to nitrogen deposition since preindustrial times via atmosphere-ecosystem exchange. We examine the individual processes that can be perturbed by nitrogen deposition and then affect surface ozone concentrations including biogenic VOC emissions, soil NO_x emissions, and ozone dry deposition. To evaluate the relative importance of nitrogen deposition, we also estimate the surface ozone changes driven by historical climate and land use changes which have been better constrained in recent studies as described above.

2 Model description

We combine a chemical transport model (GEOS-Chem) and a global land model (CLM) to investigate to interactions between nitrogen deposition and surface air quality. The interacting processes are given in the schematic diagram in Figure 1 as will be discussed below. Asynchronous coupling of the two models allow us to examine individual processes. We describe in this section the two models, the asynchronously coupled framework, as well as our model simulations.

2.1 The GEOS-Chem chemical transport model

We use the GEOS-Chem global chemical transport model (v9-02; http://www.geos-chem.org) to characterize the contribution of anthropogenic sources to nitrogen deposition and responses of surface ozone to changes in vegetation density (as represented by LAI) and soil NO_x emissions as will be provided by CLM. GEOS-Chem is driven by the MERRA (Modern Era Retrospective-analysis for Research and Applications) assimilated meteorological data from the NASA Global Modeling and Assimilation Office (GMAO). We run the GEOS-Chem model at a global horizontal resolution of 2° latitude by 2.5° longitude, and 47 levels in the vertical.

The GEOS-Chem model has been applied in a number of studies to simulate atmospheric nitrogen deposition (Zhang et al., 2012; Ellis et al., 2013; Zhao et al., 2015; 2017), surface ozone air quality (Zhang et al., 2011; 2014; Fu et al., 2015), and recently impacts of land use changes on atmospheric composition through biosphere-atmosphere exchange processes (Fu and Tai, 2015; Fu et al., 2016; Geddes et al., 2016; Heald and Geddes, 2016). It includes a detailed simulation of tropospheric NO_x-VOC-O_3-aerosol chemistry (Park et al., 2004; Mao et al., 2010). The model wet deposition scheme including scavenging in convective updraft and large-scale precipitation is described by Liu et al. (2001) for aerosols, and Mari et al. (2000) and Amos et al. (2012) for soluble gases. The dry deposition parameterization for gases and aerosols follows a standard big-leaf resistance-in-series model (Wesely, 1989; Zhang et al., 2001). Dry deposition velocities are calculated as a combination of aerodynamics resistance, boundary-layer resistance, and surface resistance.

We use the global anthropogenic emissions from the EDGAR (the Emissions Database for Global Atmospheric Research) v4.2 emission inventory (EDGAR, 2015), overwritten by regional inventories including EMEP (the European Monitoring and Evaluation Program) over Europe (Vestreng and Klein,

2002) and REAS-v2 (the Regional Emission in ASia) over East Asia (Kurokawa et al., 2012) with the NH_3 emission seasonality from Zhao et al. (2015). Natural sources include emissions from biomass burning, lightning, soil, and the biosphere. Here biomass burning emissions are from the GFED-v3 (the Global Fire Emissions Database version 3) emission inventory (van der Werf et al., 2010). Lightning NO_x emissions, as described by Sauvage et al. (2007) and Murray et al. (2012), are calculated using the cloud top height parameterization of Price and Rind (1992) and vertical distribution of Pickering et al. (1998), and further spatially redistributed to match satellite observations of lightning flashes.

We implement the following modifications so that GEOS-Chem and CLM have harmonized land surface properties for simulating surface-atmosphere exchange processes including biogenic VOC emissions, soil NO_x emissions, and dry deposition. We follow Geddes et al. (2016) and use the 16 plant function types (PFTs) from CLM in the GEOS-Chem land module. The biogenic VOC emissions in GEOS-Chem are calculated using the MEGAN v2.1 algorithm based on emission factors of the 16 PFTs and activity factors accounting for emission responses to soil and meteorological conditions, leaf age, and LAI (Guenther et al., 2012). The original above-soil NO_x emissions in GEOS-Chem are based on the empirical parameterization of Hudman et al. (2012). In this study, we calculate the above-soil NO_x emissions in CLM (with improvements as described below and in the Supplement), and archive the values hourly for input to GEOS-Chem. The canopy reduction and emission pulsing scalars from Hudman et al. (2012) are applied to estimate the above-canopy NO_x emissions. Furthermore, we have mapped the 16 CLM PFTs to the deposition surface types of Wesely (1989) following Geddes et al. (2016) to improve the consistency in dry deposition calculation.

2.2 The Community Land Model

We use the Community Land Model (CLM v4.5; Oleson et al., 2013), the land component of the Community Earth System Model (CESM), to simulate responses of LAI and soil NO_x emissions to

enhanced atmospheric nitrogen deposition from anthropogenic sources. We run the CLM model at the resolution of 2.5° latitude by 1.9° longitude, driven by the CRU-NCEP (Climatic Research Unit (CRU)-National Centers for Environmental Prediction (NCEP)) climate forcing dataset (CRUNCEP, 2015), which combines the CRU TS3.2 monthly data and the NCEP 6-hour reanalysis data with additional data over oceans, lakes and Antarctica from Qian et al. (2006). Other model inputs such as initial conditions, surface parameters, and physiological constants are from the CESM input data repository (CESM, 2015).

The CLM model in its active biogeochemistry (BGC) mode simulates detailed terrestrial biogeophysical and biogeochemical processes such as surface energy fluxes, hydrology, and biogeochemical cycles as described by Oleson et al. (2013). Each grid cell is divided into five land units including vegetation, lake, urban, glacier, and crop. The vegetation-covered areas are further characterized by 16 PFTs, which are derived from MODIS observations to represent the present-day condition (Lawrence and Chase, 2007). The CLM v4.5 model includes a vertically resolved soil biogeochemistry scheme that considers vertical transport of soil carbon and nitrogen (Koven et al., 2013). In the model, nitrogen input to the soil mineral nitrogen pool is through atmospheric deposition and biological fixation. The mineral nitrogen can be transformed to organic nitrogen by plant uptake and immobilization, or leave the ecosystem through denitrification, leaching, and other loss processes (Oleson et al., 2013).

CLM v4.5 also includes the Century Nitrogen model of del Grosso et al. (2000), which divides the soil mineral nitrogen into NH_4^+ and NO_3^-, and calculates nitrification and denitrification rates accordingly. It allows the model to calculate the N_2O emission fluxes associated with nitrification and denitrification (del Grosso et al., 2000). We further add in the model a parameterization of soil NO_x emissions based on the NO_x and N_2O ratio as described in the Appendix. We have implemented some modifications to CLM4.5 so that the simulated soil NO_x emissions are consistent with the GEOS-Chem scheme

(Appendix, Figure S1). These modifications also slightly correct the large CLM overestimations in the vegetation LAI (Dahlin et al., 2015; Duarte et al., 2017) (Figure S2) mainly due to reduced nitrogen uptake by plant in our model..

For each CLM simulation in this study, we spin up the model for a thousand years for the soil nitrogen content to reach equilibrium using the meteorological data of 2006-2010 and present-day or preindustrial nitrogen deposition fluxes. We use the last five-year results for analysis. The CLM simulations use prescribed, constant PFT distribution and soil types. We will investigate the influences of land use change on surface ozone by a separate GEOS-Chem simulation as described below. We conduct these idealized near-equilibrium CLM simulations instead of transient simulations because terrestrial ecosystems respond slowly to the environment changes (Jones et al., 2009). Here we aim to provide a first quantitative analysis of surface ozone responses, and the near-equilibrium simulations present an estimate of the long-term influence that might occur in the future (Bala et al., 2013).

2.3 Asynchronous coupling and model experiments

As illustrated in Figure 1, reactive nitrogen emitted to the atmosphere by human activities, mainly as NH_3 and NO_x, will return to the land surface through wet and dry deposition processes. This deposited nitrogen will add into the soil mineral nitrogen content, and further enhance plant growth as well as nitrification and denitrification in the nitrogen limited areas. The influences on surface ozone occur via three main processes: increasing biogenic VOC emissions while accelerating ozone dry deposition due to plant growth (as represented by increases in LAI in this study), and perturbing soil NO_x emissions from the enhanced soil mineral nitrogen pool. Besides NO_x, soil mineral nitrogen can also release to the atmospheric as nitrous acid (HONO), which influences atmospheric oxidative capacity (Su et al., 2011). Here we do not consider the influence through HONO due to a lack of its emission parameterization and chemistry simulation in both global models used in this study.

We set up an asynchronously coupled system using GEOS-Chem and CLM to investigate the influences of nitrogen deposition on surface ozone from the individual processes and the overall effects. We first calculate the global nitrogen deposition fluxes using the GEOS-Chem model averaged for the years 2006-2010. The simulated nitrogen deposition fluxes are then fed into CLM to compute LAI and soil NO_x emissions. To quantify the perturbations induced by human activities, two sets of GEOS-Chem and CLM simulations are conducted with all anthropogenic emissions turned on or off, representing the consequences of nitrogen deposition at the present-day vs. preindustrial conditions. Anthropogenic contributions are calculated as the differences between the two simulations. Finally, the CLM-simulated LAI and soil NO_x are returned to GEOS-Chem, which completes the land-atmosphere coupling and allows us to examine the impacts of nitrogen deposition on surface ozone concentrations.

Table 1 summarizes the GEOS-Chem simulations as the final step in this study. These simulations are conducted with all anthropogenic emissions but with different LAI values and soil NO_x emissions simulated by CLM. The simulation for the present-day condition (Run_all) applies the CLM-simulated present-day LAI and soil NO_x emissions. Its differences from the simulation with natural conditions (Run_nat) estimate the overall effect of anthropogenic nitrogen deposition on surface ozone. By considering the individual processes separately (Run_VOCs, Run_soilnox, and Run_drydep), simulated ozone differences with Run_nat represent their separated effects.

To evaluate the importance of nitrogen deposition, we put our analyses in the context of comparisons with surface ozone changes driven by historical climate and land use changes. As listed in Table 2, we conduct the GEOS-Chem simulations by using the 1986-1990 MERRA fields (for comparison with the 2006-2010 fields) or the preindustrial land use data (1860 vs. the present-day condition for 2000), generally following the previous work of Fu and Tai (2015) and Heald and Geddes (2016). The impacts

of climate change on wildfire emissions (Yue et al., 2015) are not considered here.

3 Global emissions and deposition of reactive nitrogen

We first evaluate the model simulation of present-day atmospheric nitrogen deposition at the global scale. Figure 2 shows the spatial distribution of annual total NH_3 and NO_x emissions, and the percentage contribution from anthropogenic sources averaged over the years 2006-2010. Global total NH_3 and NO_x emissions are 62 Tg N a^{-1} and 54 Tg N a^{-1}, of which 69% (43 Tg N a^{-1}) and 61% (33 Tg N a^{-1}) are from anthropogenic sources. Natural emissions include those from lightning (4.8 Tg N a^{-1} as NO_x), biomass burning (4.9Tg N a^{-1} as NH_3 and 6.8 Tg N a^{-1} as NO_x), soil (5.6 Tg N a^{-1} as NH_3 and 9.4 Tg N a^{-1} as NO_x), and ocean (8.6 Tg N as NH_3). About 96% of the anthropogenic emissions are in the Northern Hemisphere. We will thus focus our analyses on the Northern Hemisphere in the study. East Asia (especially eastern China and India), Europe, and North America are the major emitting regions with high ratios of anthropogenic contribution. Over the three regions, total reactive nitrogen emissions reach more than 100 kg N ha^{-1} a^{-1}, 60 kg N ha^{-1} a^{-1} and 50 kg N ha^{-1} a^{-1}, and about 75-90% of them are from anthropogenic sources. Most reactive nitrogen is emitted as NH_3 in China and India (62% in China and 71% in India), while NO_x is more abundant in Europe and North America (61% in Europe and 62% in North America), reflecting their different levels of agricultural activities.

Figure 3 shows GEOS-Chem simulated spatial distributions of annual total (reduced + oxidized) nitrogen deposition fluxes, and percentage contributions from anthropogenic emissions averaged over 2006-2010. Global total nitrogen deposition is simulated to be 114 Tg N a^{-1}, with 59% (67 Tg N a^{-1}) from wet deposition and 41% from dry deposition. 65 Tg N (38 Tg N as NH_x and 27 Tg N as NO_y) is deposited to the continents, and the remaining 49 Tg N is deposited to the ocean. Our results are comparable with previous global model estimates of Dentener et al. (2006), and more recently, Lamarque et al. (2013) and Vet et al. (2014). Using an ensemble of 21 global chemical transport

models, Vet et al. (2014) estimated a global total nitrogen deposition of 106 Tg N a^{-1}, with 55.6% deposited over the continental non-coastal areas for 2001. Deposition patterns of reactive nitrogen show a similar spatial distribution to their emissions due to the short lifetimes. Deposition fluxes reach more than 30 kg N ha^{-1} a^{-1} in Asia (in particular China and India), and 10 kg N ha^{-1} a^{-1} in Europe and North America, in agreement with the results of Vet et al. (2014). Anthropogenic emissions contribute 71% of total nitrogen deposition to the land on a global scale. The anthropogenic contributions are greater than 50% in the Northern Hemisphere, and reach more than 70% in North America, 80% in Western Europe, and 90% in East Asia.

We compare our simulation with NH_4^+ and NO_3^- wet deposition flux measurements available for the same period of 2006-2010, including measurements from the Acid Deposition Monitoring Network in East Asia (EANET, 2015) and ten surface monitoring sites in North China from Pan et al. (2012), European Monitoring and Evaluation Program (EMEP, 2015) in Europe, and National Atmospheric Deposition Program (NADP, 2015) in North America. There is a lack of direct measurements of dry deposition fluxes (Vet et al., 2014); however, previous studies have evaluated the GEOS-Chem simulated nitrogen dry deposition fluxes over the US and China using concentration measurements from surface sites and satellites, and they showed good agreement (Zhang et al., 2012; Zhao et al., 2017).

Comparisons of measured vs. simulated wet deposition fluxes over North America, Europe, and Asia are shown in Figure 3, with the correlation efficient (r) and normalized mean bias (NMB= $\sum_{i=1}^{N}(M_i - O_i)/\sum_{i=1}^{N}O_i$) between the observed (O) and modeled (M) values over the *N* sites computed. Over the three high nitrogen depositing continents, comparisons generally show high correlation coefficients (r = 0.50-0.86) and low biases for both NH_4^+ and NO_3^- wet deposition, except for biases of -

21% for NH_4^+ wet deposition over Europe and -23% for NO_3^- over East Asia. The high negative biases are likely due to the difficulty of simulating very high deposition fluxes measured at urban sites as suggested by Zhao et al. (2017) that evaluated GEOS-Chem-estimated nitrogen deposition over China at a finer horizontal resolution. Globally, the model is able to capture the magnitudes and spatial distribution of observations with high correlation coefficients of 0.86 for NH_4^+ and 0.70 for NO_3^- and small biases of -5% for NH_4^+ and -8% for NO_3^-, providing credence to the model simulation of present-day atmospheric nitrogen deposition.

4 Impact of anthropogenic nitrogen deposition on land properties

4.1 Changes in vegetation LAI and subsequent responses

We discuss in this section the changes in ecosystem structure in terms of foliage density driven by present-day anthropogenic nitrogen deposition as simulated by CLM. Figure 4 shows the simulated present-day spatial distribution of vegetation LAI, and the perturbations due to anthropogenic nitrogen deposition calculated as the differences between CLM simulations forced by total vs. natural-only nitrogen deposition. Vegetation growth is limited by nitrogen supply over most of the globe. We find that anthropogenic nitrogen deposition enhances global net primary production (NPP) by 3.7 Pg C a^{-1}, increasing LAI over those nitrogen-limited areas. Our estimated global NPP increase is consistent with Bala et al. (2013) that used an earlier version of CLM (CLM4.0) and showed that doubling (quadrupling) nitrogen deposition from the preindustrial level would increase global NPP by 2.6 (6.8) Pg C a^{-1}. As shown in Figure 4, LAI values increase by 0.1-0.7 cm^2 cm^{-2}, 0.1-0.9 cm^2 cm^{-2}, and greater than 1.0 cm^2 cm^{-2} due to anthropogenic nitrogen deposition over the three hotspots of nitrogen deposition, North America, Europe, and East Asia, respectively. The high increases over southeastern China may also partly reflect the LAI overestimation in CLM (Supplementary Figure S2); we will discuss the associated uncertainties in the next section.

Enhancement in LAI can subsequently lead to higher biogenic VOC emissions, and also higher ozone dry deposition velocities by lowering surface resistance. As shown in Figure 4, GEOS-Chem simulates a global total isoprene emission of 474 Tg a^{-1} for the present-day condition, and anthropogenic nitrogen deposition contributes about 6.6 Tg a^{-1} (1.4 %) from the LAI enhancement. Isoprene emissions are more sensitive to LAI changes at lower LAI areas due to suppression of sunlight from dense leaves. Thus emissions over southeastern China do not show large increases despite significant LAI enhancement (0.8-1.0 cm^2 cm^{-2}), while smaller LAI changes (0.2-0.6 cm^2 cm^{-2}) over regions such as India and southeastern Brazil lead to distinct increases in isoprene emissions up to 10-15%. As for dry deposition, the deposition velocities for ozone tend to increase with increasing LAI. We estimate that anthropogenic nitrogen deposition increases ozone dry deposition velocity by about 0.02 cm s^{-1} (~8%) over eastern US and Western Europe, and 0.04 cm s^{-1} (10%) over eastern and southern Asia.

4.2 Changes in soil NO_x emissions

Figure 5 shows how addition of deposited anthropogenic nitrogen to the soil mineral nitrogen pool could perturb soil NO_x emissions. As described above, we calculate the above-soil NO_x emissions in CLM using a scaling parameterization with respect to N_2O emission fluxes associated with nitrification and denitrification. Our CLM model results estimate that anthropogenic nitrogen deposition contributes to global emissions of 45.4 Tg N a^{-1} as N_2, 1.32 Tg N as N_2O, and 2.6 Tg N as NO_x above soil. Zaehle et al. (2011) previously estimated that global N_2O emissions were increased by 0.8 Tg N a^{-1} from 1860 to 2005 due to atmospheric nitrogen deposition using transient simulations of a terrestrial land model. Our estimate (1.32 Tg N-N_2O) is reasonably higher considering we use the near-equilibrium simulations.

We estimate the present-day global above-canopy NO_x emissions to be 9.4 Tg N a^{-1} (Figure 5), and they are in good agreement with the results estimated by the GEOS-Chem soil NO_x scheme of Hudman et al.

(2012) for the same period in terms of both the global magnitude (9.3 Tg N a^{-1}) and spatial distribution (Supplementary Figure S1). 1.9 Tg N a^{-1} of the above-canopy NO_x emissions are contributed by addition of deposited anthropogenic nitrogen, and 46% of the increased emissions occur over China and India. As shown in Figure 5, anthropogenic nitrogen deposition can lead to significant increases in the soil NO_x emissions especially in the Northern Hemisphere. These increases account for 30-70% of local soil NO_x emissions over regions of China, India, the US, and Europe. There is also a strong seasonality in the enhanced soil NO_x emissions since nitrification and denitrification rates are highly dependent on surface temperature. We find that 41% (0.77 Tg N) of the emission enhancement occurs in Jun-July-August, and only 13% in December-January-February.

5 Responses of surface ozone pollution

5.1 Surface ozone concentration

We now examine the changes in surface ozone air quality as driven by the overall effect of anthropogenic nitrogen deposition, as well as the individual processes of dry deposition, biogenic VOC and soil NO_x emissions. We use the metric of daytime (08:00-18:00 local time) mean surface ozone concentration. Figure 6 and 7 show the resulting surface ozone changes in the Northern Hemisphere averaged over summer (June-July-August) and spring (March-April-May), respectively. We find overall increases in the surface ozone concentration over the globe except for some regions with high NO_x emissions. In June-July-August, the mean surface ozone changes are generally within ±3 ppbv, with about 1 ppbv increases over the southwestern US and Northern Europe, nearly 2 ppbv over India, north-central China, and northern African grassland; while about 0.5 ppbv decreases in the eastern US, and 1 ppbv decreases over North China and Western Europe. Similar patterns are found for spring (March-April-May) (Figure 7), but changes are weaker than summer.

The overall impacts of nitrogen deposition on surface ozone are buffered from their effects through

individual processes. Figure 6 and 7 also show the separated effects from changes in dry deposition, biogenic VOC emissions, and soil NO_x emissions. Increases in vegetation LAI tend to increase surface ozone concentrations due to higher biogenic VOC emissions, but are largely offset by increases in the ozone loss through higher dry deposition velocities. The net effects of two depend on the LAI values and the relative changes. For example, India as one of the regions with the largest relative changes in LAI shows higher ozone changes driven by biogenic VOC emissions than the decreases from dry deposition. Meanwhile, the ozone responses to soil NO_x emissions are nonlinear depending on whether the area is NO_x-limited or NO_x-saturated. As shown in Figure 6f, soil NO_x emission enhancements generally increase summer mean surface ozone concentrations in the Northern Hemisphere except for North China, where anthropogenic NO_x emissions are particularly large and ozone production is limited by VOC emissions as reported in recent studies (Tang et al., 2012).

One of the largest uncertainties arises from the CLM overestimation of vegetation LAI (Supplementary Figure S2). To test this uncertainty, we have conducted another set of simulations in which the GEOS-Chem model simulations use observed LAI from the MODIS satellite instrument, and the CLM-simulated present-day vs. natural LAI enhancement ratios are applied to adjust MODIS LAI to examine the contribution of anthropogenic nitrogen deposition. The resulting impacts of anthropogenic nitrogen deposition on biogenic isoprene emissions, ozone dry deposition velocities, and summer mean surface ozone concentrations are shown in Supplementary Figure S3. Using adjusted MODIS LAI would lead to larger increases in biogenic isoprene emissions from anthropogenic nitrogen deposition (globally 8.2 Tg a^{-1} with the MODIS LAI vs. 5.6 Tg a^{-1} with the CLM LAI for the year 2009), and weaker increases in dry deposition velocity. As for summer mean surface ozone, we find that the differences are minor over the globe except for southeastern China where the largest LAI overestimate in CLM occurs. Changes in summer mean surface ozone due to anthropogenic nitrogen deposition are around 0.1-2.0 ppbv with the adjusted MODIS LAI but are overall negative (up to -1.0 ppbv) with the CLM LAI over

this region, reflecting the combined effect of enhanced biogenic VOC emissions and reduced ozone dry deposition loss with lower LAI.

5.2 Comparisons with climate and land use driven surface ozone changes

We also show in Figure 6 and 7 surface ozone changes driven by historical climate (1986-1990 vs. 2006-2010) and land use (1860 vs. 2000) changes as simulated by the GEOS-Chem model. The changes for ozone dry deposition velocity, biogenic isoprene, and soil NO_x emissions are included in the Supplement (Figure S4). Surface ozone changes from the 20-year climate change show a large spatial variability with more than ±10 ppbv concentration changes in both spring and summer. The large variations are mainly driven by changes in surface temperature and other meteorological variables as found in previous studies (Camalier et al., 2007; Jacob et al., 2009; Doherty et al., 2013). The large ozone concentration increases over northern Eurasia and Africa are associated with higher temperature in 2006-2010 relative to 1986-1990, which leads to higher biogenic VOC emissions (Figure S4) and stronger ozone photochemical production rates. Meanwhile higher temperature decreases surface ozone over remote regions (ocean and deserts) due to stronger ozone loss and less PAN transported from source regions (Doherty et al., 2013). Part of the ozone differences are also associated with changes in ozone dry deposition velocities and soil NO_x emissions as driven by changes in temperature and planetary boundary layer (PBL) height (Figure S4 and S5).

The historical land use change has led to decreases in surface ozone concentrations up to 5-7 ppbv for the summer mean over most regions except for some areas in Western Europe, North China, and central Africa where there are slight increases. These results are consistent with the recent work of Heald and Geddes (2016) that investigated the impacts of changes in land types and agricultural activities on surface air quality. The land-use-induced surface ozone changes are largely caused by a shift of forest trees with high biogenic emission factors to grasslands and croplands with low emission factors from

1860 to 2000. This shift in land types has also led to changes in ozone dry deposition velocity by up to 10% due to the combined impacts of LAI changes, cropland expansion (enhancing ozone vegetation uptake), and deforestation (decreasing ozone dry deposition velocity) (Heald and Geddes, 2016).

Compared with the impacts from climate change, surface ozone changes induced by anthropogenic nitrogen deposition (±3 ppbv) are smaller on a global scale, but can be rather important at the local and regional scales. The anthropogenic nitrogen deposition induced ozone changes are usually 10% of those induced by climate change at low and middle latitudes but reach about 50% at high latitudes (e.g., Canada and Northern Europe). These values are also comparable to impacts from land use changes over regions such as the western US and India, where nearly all surface ozone concentration decreases due to historical land use changes are compensated by the increases caused by anthropogenic nitrogen deposition (0.3-1.5 ppbv over the western US and 0.5-2.3 ppbv over India).

6 Conclusions

In this study we present an exploratory study aiming to quantify the influences of anthropogenic nitrogen deposition on surface ozone air quality by using the GEOS-Chem chemical transport model asynchronously coupled with the CLM land model. Increased atmospheric nitrogen deposition from human activities can modulate plant growth and mineral nitrogen content in soil, and further affect atmospheric composition through surface-atmosphere exchange processes. We consider here three processes including biogenic VOC emissions, ozone dry deposition, and soil NO_x emissions. A combination of GEOS-Chem and CLM allows us to investigate how these processes influence surface ozone and how anthropogenic nitrogen deposition perturbs them.

We simulate in GEOS-Chem global atmospheric nitrogen deposition fluxes for the present-day and the preindustrial (natural emissions only) conditions, and then conduct near-equilibrium CLM simulations

425 with these fluxes to estimate terrestrial vegetation LAI, soil NO_x emissions, and their changes due to anthropogenic nitrogen deposition. The present-day (2006-2010) nitrogen deposition is estimated to be 114 Tg N a^{-1} with 57% (65 Tg N a^{-1}) deposited to the land, consistent with available measurements of wet deposition fluxes. Anthropogenic sources contribute 71% of the nitrogen deposition to the land on the global scale, and 70%-90% over the Northern Hemisphere continents. We find that anthropogenic
430 nitrogen deposition leads to large-scale increases in LAI as well as soil NO_x emissions over the globe. The contributions from anthropogenic nitrogen deposition are particularly high over North America, Europe, and East Asia, with local values of 5%-30% for LAI and 20%-70% for present-day soil NO_x emissions.

435 Surface ozone changes driven by anthropogenic nitrogen deposition are then identified in additional GEOS-Chem simulations with CLM-simulated LAI and soil NO_x emissions. We find that the LAI enhancement due to anthropogenic nitrogen deposition can increase biogenic VOC emissions (e.g., a 6.6 Tg increase in isoprene emissions), but also lead to higher ozone dry deposition velocities (1%-15% increases over the Northern Hemisphere continents). Surface ozone changes due to the two processes
440 are largely offset. Anthropogenic nitrogen deposition also leads to general increases in soil NO_x emissions that increase the seasonal mean surface ozone concentrations over the globe except for North China where ozone production is found to be NO_x saturated. We find that the net effects of anthropogenic nitrogen deposition lead to summer mean surface ozone increases of 1 ppbv over the southwestern US, 2 ppbv over India, north-central China; while decreases of 0.5 ppbv in the eastern US,
445 and 1 ppbv over North China and Western Europe.

To assess the importance of deposited anthropogenic nitrogen influences, we also estimate surface ozone changes driven by the past 20-year climate change (from 1986-1990 to 2006-2010) and historical land use change (from 1860 to 2000). The 20-year climate change has led to large changes in the

seasonal mean surface ozone concentration (±10 ppbv), mainly driven by changes in temperature and other meteorological variables, while the historical land use change induces decreases of summer mean surface ozone by up to 5-7 ppbv in the Northern Hemisphere due to deforestation and cropland expansion as discussed in recent studies (Fu and Tai, 2015; Heald and Geddes, 2016). Compared with those changes, we find that the influences of anthropogenic nitrogen deposition can be comparable at regional scales. In particular, they may largely offset the surface ozone reduction due to historical land use change over the Northern Hemisphere continents.

While our study points out that anthropogenic nitrogen deposition can be important in modulating the surface ozone air quality, it shall be acknowledged that considerable uncertainties still exist. The estimated surface ozone responses rely heavily on the parameterizations of surface-atmosphere exchange processes. Using different parameterizations with different meteorological data, large ranges have been found for the estimates of biogenic emissions (Guenther et al., 2012; Henrot et al., 2016), soil NO_x emissions (Hudman et al., 2012), and ozone dry deposition velocities (Hardacre et al., 2015). Future work is needed to reconcile them especially in light of more observations of these emission and deposition fluxes and understand the uncertainty ranges.. The near-equilibrium CLM simulations applied in this study also imply that our estimates represent a long-term, steady-state impact, and may represent quite different results from the transient responses to actual perturbations of the terrestrial nitrogen cycle over centurial timescales. In addition, previous studies have shown that nitrogen deposition can lead to reduction of plant diversity (Sutton et al., 2014). This is not considered in our study since we use prescribed, constant PFT distribution, soil types and soil pH. All the possible uncertainties reflect the complexity in the biosphere-atmosphere interactions and feedbacks, and require future efforts in better characterizing these exchange processes in finer integrated models such as Earth system models.

Data availability

The datasets including measurements and model simulations can be accessed from websites listed in the references, downloaded from the webpage (http://www.phy.pku.edu.cn/~atmoscc/data/acp-2017-242-data.html), or by contacting the corresponding author (Lin Zhang; zhanglg@pku.edu.cn)

Appendix A

The section describes modifications we implemented to the CLM v4.5 model for better simulating the soil NO_x emissions and also reducing the model LAI overestimation. These include addition of soil NO_x emission and NH_3 volatilization processes, and an improved parameterization of nitrogen uptake by plants. We evaluate the CLM simulated results with satellite LAI observations and soil NO_x emissions calculated by GEOS-Chem.

A1 Soil NO_x emissions

The original CLM4.5 model does not estimate NO_x emissions from soil. Here we implement a process-based parameterization of soil NO_x emission as described by Parton et al. (2001). This parameterization has been recently applied to the land model LM3V-N (Huang et al., 2015). In the parameterization, soil NO_x from nitrification and denitrification is estimated based on the NO_x over N_2O emission ratio, which varies with the gas diffusivity (D/D_0) as described by the arctangent (ATAN) function (Parton et al., 2001).

$$R_{NO_x:N_2O} = 15.2 + \frac{35.4 \times \mathrm{ATAN}\left[0.68 \times \pi \times \left(10 \times \frac{D}{D_0} - 1.86\right)\right]}{\pi} \qquad \text{(A1)}$$

And the gas diffusivity is calculated as a function of air filled porosity (AFPS) (Davidson and Trumbore, 1995):

$$\frac{D}{D_0} = 0.209 \times \mathrm{AFPS}^{\frac{4}{3}} \qquad \text{(A2)}$$

Above-soil NO_x emissions are thus derived from soil N_2O emissions as already estimated in CLM4.5 and the $R_{NO_x:N_2O}$ ratios. However, we find that soil NO_x emissions derived from the original CLM and this parameterization show a distinctly different spatial pattern from those calculated in GEOS-Chem with the scheme of Hudman et al. (2012) (Figure S1). To improve the consistency, we also add the process of NH_3 volatilization and update the parameterization of plant nitrogen uptake in the model as described in the sections below. In addition, we have implemented a soil temperature (T_{soil}) dependent factor (the equation below) from Xu and Prentice (2008) to the N_2O and N_2 emission ratio to reduce the CLM high soil NO_x emissions at high latitudes.

$$f(T_{soil}) = \exp(308.56 \times (\frac{1}{68.02} - \frac{1}{T_{soil} + 46.02})) \quad \text{(A3)}$$

A2 NH_3 volatilization

NH_3 is highly volatile under high soil temperature and pH conditions. The original CLM calculates abnormally high soil NH_4^+ content over deserts (e.g., more than 20 g N m^2 in Sahara) due to a lack of the NH_3 volatilization process. Here we implement a process-based NH_3 volatilization parameterization in CLM following Xu and Prentice (2008). NH_3 volatilization from soil (V_NH_3) is estimated as a function of water filled pore space (WFPS), soil pH, and temperature (T_{soil}) given below.

$$V\_NH_3 = f(pH) f(T_{soil}) (1 - WFPS) \frac{N_{NH_4^+}}{b_{NH_4^+}} \quad \text{(A4)}$$

where $N_{NH_4^+}$ is the soil NH_4^+ content and $b_{NH_4^+}$ is the buffer parameter for NH_4^+ (10 as given by Huang et al. (2015)). The soil pH factor $f(pH)$ and soil temperature factor $f(T_{soil})$ are given below:

$$f(pH) = e^{2 \times (pH - 10)} \quad \text{(A5)}$$

$$f(T_{soil}) = \min(1, e^{308.56 \times (\frac{1}{71.02} - \frac{1}{T_{soil} + 46.02})}) \quad \text{(A6)}$$

This NH_3 volatilization parameterization corrects the CLM bias in the soil NH_4^+ concentration over desert areas, and show consistent results with Xu and Prentice (2008).

A3 Plant nitrogen uptake

In the original CLM4.5, nitrogen uptake by plants is estimated as plant demand as long as there is sufficient nitrogen supply. However, many factors may influence plant nitrogen uptake, such as soil inorganic nitrogen concentration, the fine root mass, and soil temperature. Here we follow Thomas et al. (2013) and calculate in CLM the plant nitrogen uptake capacity ($U_{n,plant}$) based on the Hanes Woolf Mechanism:

$$U_{n,plant} = V_{n,max}\frac{NH_{4,av} + NO_{3,av}}{(NH_{4,av} + NO_{3,av}) + K_{min}}C_{root}f(T_{soil}) \qquad (A7)$$

where $V_{n,max}$ =2.7x10^{-8} g N g C^{-1} s^{-1} is the maximum N uptake per unit fine root C at 25°C; $NH_{4,av}$ and $NO_{3,av}$ are available mineral NH_4^+ and NO_3^- in the soil; K_{min}=0.83 g N m^{-2} is the half saturation concentration of fine root nitrogen uptake from Kronzucker et al. (1995; 1996), C_{root} is fine root carbon concentration (g C m^{-2}), and *f*(Tsoil) represents a function of limitation of soil temperature on plant nitrogen uptake as described in Thomas et al. (2013). The calculated uptake capacity is then compared to the plant demand, and the smaller one defines the plant uptake of mineral nitrogen in the modified CLM.

Acknowledgments

This work was supported by the National Key R&D Program of China (2017YFC0210102), China's National Basic Research Program (2014CB441303), and the National Natural Science Foundation of China (41205103, 41475112, and 41405144). The collaboration was also supported by the General Research Fund (project #: 14323116) of the Research Grants Council of Hong Kong given to Amos P.

K. Tai.

5 Figures are included in the supplement related to this article.

References

Acid Deposition Monitoring Network in East Asia (EANET), http://www.eanet.asia/index.html, 2015.

Ainsworth, E. A., Yendrek, C. R., Sitch, S., Collins, W. J., and Emberson, L. D.: The effects of tropospheric ozone on net primary productivity and implications for climate change, Annual review of plant biology, 63, 637-661, 2012.

Amos, H. M., Jacob, D. J., Holmes, C. D., Fisher, J. A., Wang, Q., Yantosca, R. M., Corbitt, E. S., Galarneau, E., Rutter, A. P., Gustin, M. S., Steffen, A., Schauer, J. J., Graydon, J. A., Louis, V. L. S., Talbot, R. W., Edgerton, E. S., Zhang, Y., and Sunderland, E. M.: Gas-particle partitioning of atmospheric Hg(II) and its effect on global mercury deposition, Atmos. Chem. Phys., 12, 591-603, doi: 10.5194/acp-12-591-2012, 2012.

Avnery, S., Mauzerall, D. L., Liu, J., and Horowitz, L. W.: Global crop yield reductions due to surface ozone exposure: 1. Year 2000 crop production losses and economic damage, Atmos. Environ., 45, 2284-2296, 2011.

Bala, G., Devaraju, N., Chaturvedi, R. K., Caldeira, K., and Nemani, R.: Nitrogen deposition: how important is it for global terrestrial carbon uptake?, Biogeosciences, 10, 7147-7160, doi: 10.5194/bg-10-7147-2013, 2013.

Baron, J. S., Barber, M., Adams, M., Agboola, J. I., Allen, E. B., Bealey, W. J., Bobbink, R., Bobrovsky, M. V., Bowman, W. D., Branquinho, C., Bustamente, M. M. C., Clark, C. M., Cocking, E. C., Cruz, C., Davidson, E., Denmead, O. T., Dias, T., Dise, N. B., Feest, A., Galloway, J. N., Geiser, L. H., Gilliam, F. S., Harrison, I. J., Khanina, L. G., Lu, X., Manrique, E., Hueso, R. O., Ometto, J. P. H. B., Payne, R., Scheuschner, T., Sheppard, L. J., Simpson, G. L., Singh, Y. V., Stevens, C. J., Strachan, I., Sverdrup, H., Tokuchi, N., Dobben, H. v., and Woodin, S.: The Effects of Atmospheric Nitrogen Deposition on Terrestrial and Freshwater Biodiversity, in: Nitrogen Deposition, Critical Loads and Biodiversity, edited by: Sutton, M. A., Mason, K. E., Sheppard, L. J., Sverdrup, H., Haeuber, R., and Hicks, W. K., Springer Netherlands, Dordrecht, 465-480, 2014.

Bates, D. V.: Ambient Ozone and Mortality, Epidemiology, 16, 427-429, doi: 10.1097/01.ede.0000165793.71278.ec, 2005.

Camalier, L., Cox, W., and Dolwick, P.: The effects of meteorology on ozone in urban areas and their use in assessing ozone trends, Atmos. Environ., 41, 7127-7137, 2007.

Climatic Research Unit (CRU)-National Centers for Environmental Prediction (NCEP) (CRUNCEP), data available at http://dods.extra.cea.fr/store/p529viov/cruncep/V4_1901_2011/, 2015.

Community Earth System Model (CESM) input data repository, data available at https://svn-ccsm-inputdata.cgd.ucar.edu/trunk/inputdata/, 2015.

Dahlin, K. M., Fisher, R. A., and Lawrence, P. J.: Environmental drivers of drought deciduous phenology in the Community Land Model, Biogeosciences, 12, 5061-5074, doi: 10.5194/bg-12-5061-2015, 2015.

Davidson, E. A., and Trumbore, S. E.: Gas diffusivity and production of CO2 in deep soils of the eastern Amazon, Tellus B, 47, 550-565, doi: 10.1034/j.1600-0889.47.issue5.3.x, 1995.

Del Grosso, S. J., Parton, W. J., Mosier, A. R., Ojima, D. S., Kulmala, A. E., and Phongpan, S.: General model for N_2O and N_2 gas emissions from soils due to dentrification, Global Biogeochem. Cy., 14, 1045-1060, doi: 10.1029/1999GB001225, 2000.

Dentener, F., Drevet, J., Lamarque, J. F., Bey, I., Eickhout, B., Fiore, A. M., Hauglustaine, D., Horowitz, L. W., Krol, M., Kulshrestha, U. C., Lawrence, M., Galy-Lacaux, C., Rast, S., Shindell, D., Stevenson, D., Van Noije, T., Atherton, C., Bell, N., Bergman, D., Butler, T., Cofala, J., Collins, B., Doherty, R., Ellingsen, K., Galloway, J., Gauss, M., Montanaro, V., Müller, J. F., Pitari, G., Rodriguez, J., Sanderson, M., Solmon, F., Strahan, S., Schultz, M., Sudo, K., Szopa, S., and Wild, O.: Nitrogen and sulfur deposition on regional and global scales: A multimodel evaluation, Global Biogeochem. Cy., 20, GB4003, doi: 10.1029/2005GB002672, 2006.

Doherty, R. M., Wild, O., Shindell, D. T., Zeng, G., MacKenzie, I. A., Collins, W. J., Fiore, A. M., Stevenson, D. S., Dentener, F. J., Schultz, M. G., Hess, P., Derwent, R. G., and Keating, T. J.: Impacts of climate change on surface ozone and intercontinental ozone pollution: A multi-model study, J. Geophys. Res.-Atmos, 118, 3744-3763, doi: 10.1002/jgrd.50266, 2013.

Duarte, H. F., Raczka, B. M., Ricciuto, D. M., Lin, J. C., Koven, C. D., Thornton, P. E., Bowling, D. R., Lai, C. T., Bible, K. J., and Ehleringer, J. R.: Evaluating the Community Land Model (CLM 4.5) at a Coniferous Forest Site in Northwestern United States Using Flux and Carbon-Isotope Measurements, Biogeosciences Discuss., 2016, 1-35, doi: 10.5194/bg-2016-441, 2016.

Duce, R. A., LaRoche, J., Altieri, K., Arrigo, K. R., Baker, A. R., Capone, D. G., Cornell, S., Dentener, F., Galloway, J., Ganeshram, R. S., Geider, R. J., Jickells, T., Kuypers, M. M., Langlois, R., Liss, P. S., Liu, S. M., Middelburg, J. J., Moore, C. M., Nickovic, S., Oschlies, A., Pedersen, T., Prospero, J., Schlitzer, R., Seitzinger, S., Sorensen, L. L., Uematsu, M., Ulloa, O., Voss, M., Ward, B., and Zamora, L.: Impacts of Atmospheric Anthropogenic Nitrogen on the Open Ocean, Science, 320, 893-897, doi: 10.1126/science.1150369, 2008.

Ellis, R. A., Jacob, D. J., Sulprizio, M. P., Zhang, L., Holmes, C. D., Schichtel, B. A., Blett, T., Porter, E., Pardo, L. H., and Lynch, J. A.: Present and future nitrogen deposition to national parks in the United States: critical load exceedances, Atmos. Chem. Phys., 13, 9083-9095, doi: 10.5194/acp-13-9083-2013, 2013.

European Monitoring and Evaluation Program (EMEP), http://www.nilu.no/projects/ccc/emepdata.html, 2015.

Fowler, D., Pilegaard, K., Sutton, M. A., Ambus, P., Raivonen, M., Duyzer, J., Simpson, D., Fagerli, H., Fuzzi, S., Schjoerring, J. K., Granier, C., Neftel, A., Isaksen, I. S. A., Laj, P., Maione, M., Monks, P. S., Burkhardt, J., Daemmgen, U., Neirynck, J., Personne, E., Wichink-Kruit, R., Butterbach-Bahl, K., Flechard, C., Tuovinen, J. P., Coyle, M., Gerosa, G., Loubet, B., Altimir, N., Gruenhage, L., Ammann, C., Cieslik, S., Paoletti, E., Mikkelsen, T. N., Ro-Poulsen, H., Cellier, P., Cape, J. N., Horváth, L., Loreto, F., Niinemets, Ü., Palmer, P. I., Rinne, J., Misztal, P., Nemitz, E., Nilsson, D., Pryor, S., Gallagher, M. W., Vesala, T., Skiba, U., Brüggemann, N., Zechmeister-Boltenstern, S., Williams, J., O'Dowd, C., Facchini, M. C., de Leeuw, G., Flossman, A., Chaumerliac, N., and Erisman, J. W.: Atmospheric composition change: Ecosystems–Atmosphere interactions, Atmos. Environ., 43, 5193-5267, 2009.

Fowler, D., Coyle, M., Skiba, U., Sutton, M. A., Cape, J. N., Reis, S., Sheppard, L. J., Jenkins, A., Grizzetti, B., Galloway, J. N., Vitousek, P., Leach, A., Bouwman, A. F., Butterbach-Bahl, K., Dentener, F., Stevenson, D., Amann, M., and Voss, M.: The global nitrogen cycle in the twenty-first century, Philosophical Transactions of the Royal Society B: Biological Sciences, 368, 2621, doi: 10.1098/rstb.2013.0164, 2013.

Fu, T.-M., Zheng, Y., Paulot, F., Mao, J., and Yantosca, R. M.: Positive but variable sensitivity of August surface ozone to large-scale warming in the southeast United States, Nature Clim. Change, 5, 454-458, doi: 10.1038/nclimate2567, 2015.

Fu, Y., and Tai, A. P. K.: Impact of climate and land cover changes on tropospheric ozone air quality and public health in East Asia between 1980 and 2010, Atmos. Chem. Phys., 15, 10093-10106, doi: 10.5194/acp-15-10093-2015, 2015.

Fu, Y., Tai, A. P. K., and Liao, H.: Impacts of historical climate and land cover changes on fine particulate matter (PM2.5) air quality in East Asia between 1980 and 2010, Atmos. Chem. Phys., 16, 10369-10383, doi: 10.5194/acp-16-10369-2016, 2016.

Galloway, J. N., Dentener, F. J., Capone, D. G., Boyer, E. W., Howarth, R. W., Seitzinger, S. P., Asner, G. P., Cleveland, C. C., Green, P. A., Holland, E. A., Karl, D. M., Michaels, A. F., Porter, J. H., Townsend, A. R., and Vöosmarty, C. J.: Nitrogen Cycles: Past, Present, and Future, Biogeochemistry, 70, 153-226, doi: 10.1007/s10533-004-0370-0, 2004.

Geddes, J. A., Heald, C. L., Silva, S. J., and Martin, R. V.: Land cover change impacts on atmospheric chemistry: simulating projected large-scale tree mortality in the United States, Atmos. Chem. Phys., 16, 2323-2340, doi: 10.5194/acp-16-2323-2016, 2016.

Guenther, A. B., Jiang, X., Heald, C. L., Sakulyanontvittaya, T., Duhl, T., Emmons, L. K., and Wang, X.: The Model of Emissions of Gases and Aerosols from Nature version 2.1 (MEGAN2.1): an extended and updated framework for modeling biogenic emissions, Geosci. Model Dev., 5, 1471-1492, doi: 10.5194/gmd-5-1471-2012, 2012.

Hardacre, C., Wild, O., and Emberson, L.: An evaluation of ozone dry deposition in global scale chemistry climate models, Atmos. Chem. Phys., 15, 6419-6436, doi: 10.5194/acp-15-6419-2015,

2015.

Heald, C. L., and Geddes, J. A.: The impact of historical land use change from 1850 to 2000 on secondary particulate matter and ozone, Atmos. Chem. Phys., 16, 14997-15010, doi: 10.5194/acp-16-14997-2016, 2016.

Henrot, A. J., Stanelle, T., Schröder, S., Siegenthaler, C., Taraborrelli, D., and Schultz, M. G.: Implementation of the MEGAN (v2.1) biogenic emission model in the ECHAM6-HAMMOZ chemistry climate model, Geosci. Model Dev., 10, 903-926, doi: 10.5194/gmd-10-903-2017, 2017.

Huang, Y., and Gerber, S.: Global soil nitrous oxide emissions in a dynamic carbon-nitrogen model, Biogeosciences, 12, 6405-6427, doi: 10.5194/bg-12-6405-2015, 2015.

Hudman, R. C., Moore, N. E., Mebust, A. K., Martin, R. V., Russell, A. R., Valin, L. C., and Cohen, R. C.: Steps towards a mechanistic model of global soil nitric oxide emissions: implementation and space based-constraints, Atmos. Chem. Phys., 12, 7779-7795, doi: 10.5194/acp-12-7779-2012, 2012.

Jacob, D. J., and Winner, D. A.: Effect of climate change on air quality, Atmos. Environ., 43, 51-63, 2009.

Jerrett , M., Burnett , R. T., Pope , C. A. I., Ito , K., Thurston , G., Krewski , D., Shi , Y., Calle , E., and Thun , M.: Long-Term Ozone Exposure and Mortality, New England Journal of Medicine, 360, 1085-1095, 2009.

Jones, C., Lowe, J., Liddicoat, S., and Betts, R.: Committed terrestrial ecosystem changes due to climate change, Nature Geosci, 2, 484-487, doi: 10.1038/ngeo555, 2009.

Koven, C. D., Riley, W. J., Subin, Z. M., Tang, J. Y., Torn, M. S., Collins, W. D., Bonan, G. B., Lawrence, D. M., and Swenson, S. C.: The effect of vertically resolved soil biogeochemistry and alternate soil C and N models on C dynamics of CLM4, Biogeosciences, 10, 7109-7131, doi: 10.5194/bg-10-7109-2013, 2013.

Kronzucker, H. J., Siddiqi, M. Y., and Glass, A.: Kinetics of NO3- Influx in Spruce, Plant Physiology, 109, 319-326, doi: 10.1104/pp.109.1.319, 1995.

Kronzucker, H. J., Siddiqi, M. Y., and Glass, A.: Kinetics of NH4+ Influx in Spruce, Plant Physiology, 110, 773-779, doi: 10.1104/pp.110.3.773, 1996.

Kurokawa, J., Ohara, T., Morikawa, T., Hanayama, S., Janssens-Maenhout, G., Fukui, T., Kawashima, K., and Akimoto, H.: Emissions of air pollutants and greenhouse gases over Asian regions during 2000–2008: Regional Emission inventory in ASia (REAS) version 2, Atmos. Chem. Phys., 13, 11019-11058, doi: 10.5194/acp-13-11019-2013, 2013.

Lamarque, J. F., Dentener, F., McConnell, J., Ro, C. U., Shaw, M., Vet, R., Bergmann, D., Cameron-Smith, P., Dalsoren, S., Doherty, R., Faluvegi, G., Ghan, S. J., Josse, B., Lee, Y. H., MacKenzie, I. A., Plummer, D., Shindell, D. T., Skeie, R. B., Stevenson, D. S., Strode, S., Zeng, G., Curran, M., Dahl-Jensen, D., Das, S., Fritzsche, D., and Nolan, M.: Multi-model mean nitrogen and sulfur deposition from the Atmospheric Chemistry and Climate Model Intercomparison Project (ACCMIP): evaluation of historical and projected future changes, Atmos. Chem. Phys., 13, 7997-8018, doi:

10.5194/acp-13-7997-2013, 2013.

Lawrence, P. J., and Chase, T. N.: Representing a new MODIS consistent land surface in the Community Land Model (CLM 3.0), J. Geophys. Res.-Biogeo., 112, G01023, 10.1029/2006JG000168, 2007.

Liu, H., Jacob, D. J., Bey, I., and Yantosca, R. M.: Constraints from 210Pb and 7Be on wet deposition and transport in a global three-dimensional chemical tracer model driven by assimilated meteorological fields, J. Geophys. Res.-Atmos, 106, 12109-12128, doi: 10.1029/2000JD900839, 2001.

Liu, L., and Greaver, T. L.: A review of nitrogen enrichment effects on three biogenic GHGs: the CO_2 sink may be largely offset by stimulated N_2O and CH_4 emission, Ecology Letters, 12, 1103-1117, 2009.

Liu, X., Zhang, Y., Han, W., Tang, A., Shen, J., Cui, Z., Vitousek, P., Erisman, J. W., Goulding, K., Christie, P., Fangmeier, A., and Zhang, F.: Enhanced nitrogen deposition over China, Nature, 494, 459-462, doi: 10.1038/nature11917, 2013.

Lu, X., Mao, Q., Gilliam, F. S., Luo, Y., and Mo, J.: Nitrogen deposition contributes to soil acidification in tropical ecosystems, Global Change Biology, 20, 3790-3801, 2014.

Mao, J., Jacob, D. J., Evans, M. J., Olson, J. R., Ren, X., Brune, W. H., Clair, J. M. S., Crounse, J. D., Spencer, K. M., Beaver, M. R., Wennberg, P. O., Cubison, M. J., Jimenez, J. L., Fried, A., Weibring, P., Walega, J. G., Hall, S. R., Weinheimer, A. J., Cohen, R. C., Chen, G., Crawford, J. H., McNaughton, C., Clarke, A. D., Jaeglé, L., Fisher, J. A., Yantosca, R. M., Le Sager, P., and Carouge, C.: Chemistry of hydrogen oxide radicals (HO_x) in the Arctic troposphere in spring, Atmos. Chem. Phys., 10, 5823-5838, doi: 10.5194/acp-10-5823-2010, 2010.

Mari, C., Jacob, D. J., and Bechtold, P.: Transport and scavenging of soluble gases in a deep convective cloud, J. Geophys. Res.-Atmos, 105, 22255-22267, doi: 10.1029/2000JD900211, 2000.

Matyssek, R., Karnosky, D. F., Wieser, G., Percy, K., Oksanen, E., Grams, T. E. E., Kubiske, M., Hanke, D., and Pretzsch, H.: Advances in understanding ozone impact on forest trees: Messages from novel phytotron and free-air fumigation studies, Environmental Pollution, 158, 1990-2006, 2010.

Mills, G., Buse, A., Gimeno, B., Bermejo, V., Holland, M., Emberson, L., and Pleijel, H.: A synthesis of AOT40-based response functions and critical levels of ozone for agricultural and horticultural crops, Atmos. Environ., 41, 2630-2643, 2007.

Murray, L. T., Jacob, D. J., Logan, J. A., Hudman, R. C., and Koshak, W. J.: Optimized regional and interannual variability of lightning in a global chemical transport model constrained by LIS/OTD satellite data, J. Geophys. Res.-Atmos, 117, D20307 doi: 10.1029/2012JD017934, 2012.

National Acid Deposition Program (NADP), http://nadp.sws.uiuc.edu/, 2015.

Oleson, K., Lawrence, D., Bonan, G., Drewniak, B., Huang, M., Koven, C., Levis, S., Li, F., Riley, W., Subin, Z., S.C, S., P.E, T., A, B., R, F., E, K., J.-F, L., P.J, L., L.R, L., W, L., S, M., D.M, R., W, S.,

Y, S., J, T., and Z.-L, Y.: Technical Description of version 4.5 of the Community Land Model (CLM). Ncar Technical Note NCAR/TN-503+STR, National Center for Atmospheric Research, 422pp, doi: 10.5065/D6RR1W7M, 2013.

Pan, Y. P., Wang, Y. S., Tang, G. Q., and Wu, D.: Wet and dry deposition of atmospheric nitrogen at ten sites in Northern China, Atmos. Chem. Phys., 12, 6515-6535, doi: 10.5194/acp-12-6515-2012, 2012.

Pan, Y., Tian, S., Liu, D., Fang, Y., Zhu, X., Zhang, Q., Zheng, B., Michalski, G., and Wang, Y.: Fossil fuel combustion-related emissions dominate atmospheric ammonia sources during severe haze episodes: evidence from 15N-stable isotope in size-resolved aerosol ammonium, Environ. Sci. Technol, 50, 8049-8056, 2016.

Park, R. J., Jacob, D. J., Field, B. D., Yantosca, R. M., and Chin, M.: Natural and transboundary pollution influences on sulfate-nitrate-ammonium aerosols in the United States: Implications for policy, J. Geophys. Res.-Atmos, 109, D15204, doi: 10.1029/2003JD004473, 2004.

Parton, W. J., Holland, E. A., Del Grosso, S. J., Hartman, M. D., Martin, R. E., Mosier, A. R., Ojima, D. S., and Schimel, D. S.: Generalized model for NO x and N_2O emissions from soils, Journal of Geophysical Research: Atmospheres, 106, 17403-17419, doi: 10.1029/2001JD900101, 2001.

Pickering, K. E., Wang, Y., Tao, W.-K., Price, C., and Müller, J.-F.: Vertical distributions of lightning NOx for use in regional and global chemical transport models, J. Geophys. Res.-Atmos, 103, 31203-31216, doi: 10.1029/98JD02651, 1998.

Price, C., and Rind, D.: A simple lightning parameterization for calculating global lightning distributions, J. Geophys. Res.-Atmos, 97, 9919-9933, doi: 10.1029/92JD00719, 1992.

Qian, T., Dai, A., Trenberth, K. E., and Oleson, K. W.: Simulation of Global Land Surface Conditions from 1948 to 2004. Part I: Forcing Data and Evaluations, Journal of Hydrometeorology, 7, 953-975, 2006.

Rodríguez, L., and Macías, F.: Eutrophication trends in forest soils in Galicia (NW Spain) caused by the atmospheric deposition of nitrogen compounds, Chemosphere, 63, 1598-1609, 2006.

Sadiq, M., Tai, A. P. K., Lombardozzi, D., and Val Martin, M.: Effects of ozone–vegetation coupling on surface ozone air quality via biogeochemical and meteorological feedbacks, Atmos. Chem. Phys., 17, 3055-3066, doi: 10.5194/acp-17-3055-2017, 2017.

Sauvage, B., Martin, R. V., van Donkelaar, A., Liu, X., Chance, K., Jaeglé, L., Palmer, P. I., Wu, S., and Fu, T. M.: Remote sensed and in situ constraints on processes affecting tropical tropospheric ozone, Atmos. Chem. Phys., 7, 815-838, doi: 10.5194/acp-7-815-2007, 2007.

Stevens, C. J., Maskell, L. C., Smart, S. M., Caporn, S. J. M., Dise, N. B., and Gowing, D. J. G.: Identifying indicators of atmospheric nitrogen deposition impacts in acid grasslands, Biological Conservation, 142, 2069-2075, 2009.

Su, H., Cheng, Y., Oswald, R., Behrendt, T., Trebs, I., Meixner, F. X., Andreae, M. O., Cheng, P., Zhang, Y., and Pöschl, U.: Soil Nitrite as a Source of Atmospheric HONO and OH Radicals,

Science, 333, 1616-1618, doi: 10.1126/science.1207687, 2011.

Sutton, M. A., Mason, K. E., Sheppard, L. J., Sverdrup, H., Haeuber, R., and Hicks, W. K.: Nitrogen deposition, critical loads and biodiversity, Springer Science & Business Media, 535 pp., 2014.

Tai, A. P. K., Martin, M. V., and Heald, C. L.: Threat to future global food security from climate change and ozone air pollution, Nature Clim. Change, 4, 817-821, doi: 10.1038/nclimate2317, 2014.

Tang, G., Wang, Y., Li, X., Ji, D., Hsu, S., and Gao, X.: Spatial-temporal variations in surface ozone in Northern China as observed during 2009–2010 and possible implications for future air quality control strategies, Atmos. Chem. Phys., 12, 2757-2776, doi: 10.5194/acp-12-2757-2012, 2012.

Thomas, R. Q., Bonan, G. B., and Goodale, C. L.: Insights into mechanisms governing forest carbon response to nitrogen deposition: a model–data comparison using observed responses to nitrogen addition, Biogeosciences, 10, 3869-3887, doi: 10.5194/bg-10-3869-2013, 2013.

Val Martin, M., Heald, C. L., Lamarque, J.-F., Tilmes, S., Emmons, L. K., and Schichtel, B. A.: How emissions, climate, and land use change will impact mid-century air quality over the United States: a focus on effects at national parks, Atmos. Chem. Phys., 15, 2805-2823, doi:10.5194/acp-15-2805-2015, 2015.

van der Werf, G. R., Randerson, J. T., Giglio, L., Collatz, G. J., Mu, M., Kasibhatla, P. S., Morton, D. C., DeFries, R. S., Jin, Y., and van Leeuwen, T. T.: Global fire emissions and the contribution of deforestation, savanna, forest, agricultural, and peat fires (1997–2009), Atmos. Chem. Phys., 10, 11707-11735, doi: 10.5194/acp-10-11707-2010, 2010.

Vestreng, V., and Klein, H.: Emission data reported to UNECE/EMEP: Quality assurance and trend analysis & Presentation of WebDab, Det norske meterologiske institutt, 2002.

Vet, R., Artz, R. S., Carou, S., Shaw, M., Ro, C.-U., Aas, W., Baker, A., Bowersox, V. C., Dentener, F., Galy-Lacaux, C., Hou, A., Pienaar, J. J., Gillett, R., Forti, M. C., Gromov, S., Hara, H., Khodzher, T., Mahowald, N. M., Nickovic, S., Rao, P. S. P., and Reid, N. W.: A global assessment of precipitation chemistry and deposition of sulfur, nitrogen, sea salt, base cations, organic acids, acidity and pH, and phosphorus, Atmos. Environ., 93, 3-100, 2014.

Wesely, M. L.: Parameterization of surface resistances to gaseous dry deposition in regional-scale numerical models, Atmos. Environ., 23, 1293-1304, 1989.

Xu, R. I., and Prentice, I. C.: Terrestrial nitrogen cycle simulation with a dynamic global vegetation model, Global Change Biology, 14, 1745-1764, doi: 10.1111/j.1365-2486.2008.01625.x, 2008.

Young, P. J., Archibald, A. T., Bowman, K. W., Lamarque, J. F., Naik, V., Stevenson, D. S., Tilmes, S., Voulgarakis, A., Wild, O., Bergmann, D., Cameron-Smith, P., Cionni, I., Collins, W. J., Dalsøren, S. B., Doherty, R. M., Eyring, V., Faluvegi, G., Horowitz, L. W., Josse, B., Lee, Y. H., MacKenzie, I. A., Nagashima, T., Plummer, D. A., Righi, M., Rumbold, S. T., Skeie, R. B., Shindell, D. T., Strode, S. A., Sudo, K., Szopa, S., and Zeng, G.: Pre-industrial to end 21st century projections of tropospheric ozone from the Atmospheric Chemistry and Climate Model Intercomparison Project (ACCMIP), Atmos. Chem. Phys., 13, 2063-2090, doi: 10.5194/acp-13-2063-2013, 2013.

Yue, X., and Unger, N.: Ozone vegetation damage effects on gross primary productivity in the United States, Atmos. Chem. Phys., 14, 9137-9153, doi: 10.5194/acp-14-9137-2014, 2014.

Yue, X., Mickley, L. J., Logan, J. A., Hudman, R. C., Martin, M. V., and Yantosca, R. M.: Impact of 2050 climate change on North American wildfire: consequences for ozone air quality, Atmos. Chem. Phys., 15, 10033-10055, doi: 10.5194/acp-15-10033-2015, 2015.

Yue, X., Unger, N., Harper, K., Xia, X., Liao, H., Zhu, T., Xiao, J., Feng, Z., and Li, J.: Ozone and haze pollution weakens net primary productivity in China, Atmos. Chem. Phys. Discuss., 2016, 1-36, doi: 10.5194/acp-2016-1025, 2016.

Zaehle, S., Ciais, P., Friend, A. D., and Prieur, V.: Carbon benefits of anthropogenic reactive nitrogen offset by nitrous oxide emissions, Nature Geosci, 4, 601-605, doi: 10.1038/ngeo1207, 2011.

Zhang, L., Gong, S., Padro, J., and Barrie, L.: A size-segregated particle dry depo- sition scheme for an atmospheric aerosol module. Atmos. Environ. 35, 549-560, 2001.

Zhang, L., Jacob, D. J., Downey, N. V., Wood, D. A., Blewitt, D., Carouge, C. C., van Donkelaar, A., Jones, D. B. A., Murray, L. T., and Wang, Y.: Improved estimate of the policy-relevant background ozone in the United States using the GEOS-Chem global model with 1/2° × 2/3° horizontal resolution over North America, Atmos. Environ., 45, 6769-6776, 2011.

Zhang, L., Jacob, D. J., Knipping, E. M., Kumar, N., Munger, J. W., Carouge, C. C., van Donkelaar, A., Wang, Y. X., and Chen, D.: Nitrogen deposition to the United States: distribution, sources, and processes, Atmos. Chem. Phys., 12, 4539-4554, doi: 10.5194/acp-12-4539-2012, 2012.

Zhang, L., Jacob, D. J., Yue, X., Downey, N. V., Wood, D. A., and Blewitt, D.: Sources contributing to background surface ozone in the US Intermountain West, Atmos. Chem. Phys., 14, 5295-5309, doi: 10.5194/acp-14-5295-2014, 2014.

Zhang, Y., Cooper, O. R., Gaudel, A., Thompson, A. M., Nedelec, P., Ogino, S.-Y., and West, J. J.: Tropospheric ozone change from 1980 to 2010 dominated by equatorward redistribution of emissions, Nature Geosci, 9, 875-879, 2016.

Zhao, Y., Zhang, L., Pan, Y., Wang, Y., Paulot, F., and Henze, D. K.: Atmospheric nitrogen deposition to the northwestern Pacific: seasonal variation and source attribution, Atmos. Chem. Phys., 15, 10905-10924, doi: 10.5194/acp-15-10905-2015, 2015.

Zhao, Y., Zhang, L., Chen, Y., Liu, X., Xu, W., Pan, Y., and Duan, L.: Atmospheric nitrogen deposition to China: A model analysis on nitrogen budget and critical load exceedance, Atmos. Environ., 153, 32-40, 2017.

Tables

Table 1. GEOS-Chem simulations to quantify surface ozone response to nitrogen deposition from each process and the net effect[1]

	Run_all	Run_VOCs	Run_soilnox	Run_drydep	Run_nat
Biogenic VOCs	All	All	Nat	Nat	Nat
Soil NO_x	All	Nat	All	Nat	Nat
Dry deposition	All	Nat	Nat	All	Nat

[1] In the table All represents the use of CLM outputs simulated with the present-day atmospheric nitrogen deposition, and Nat represents the use of CLM outputs with natural nitrogen deposition alone. All GEOS-Chem simulations listed in the table are conducted with present-day anthropogenic and natural emissions turned on.

Table 2. GEOS-Chem simulations with the input data time listed to quantify surface ozone changes driven by historical climate and land use changes

	Run_std	Run_met	Run_land
Land use	2000	2000	1860
Meteorology	2006-2010	1986-1990	2006-2010

Figures

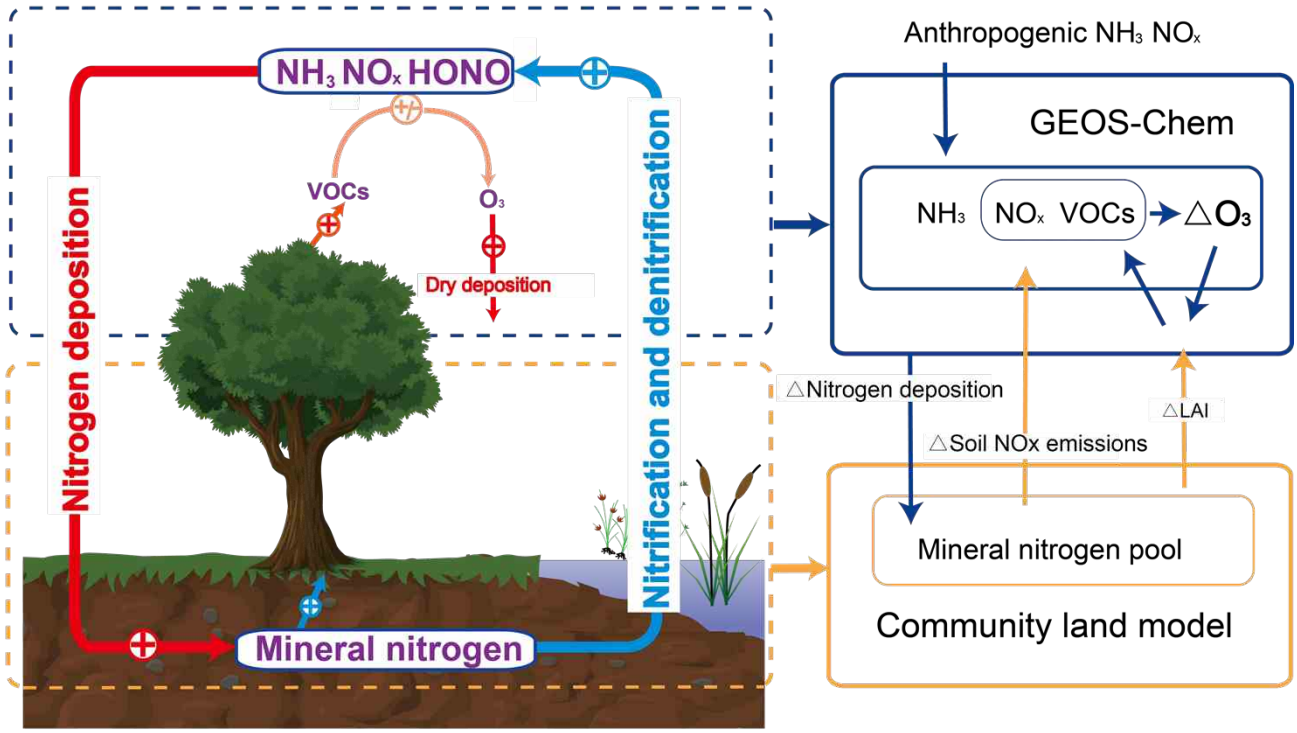

Figure 1. The schematic diagram and flowchart of the land-atmosphere asynchronously coupled system for the study.

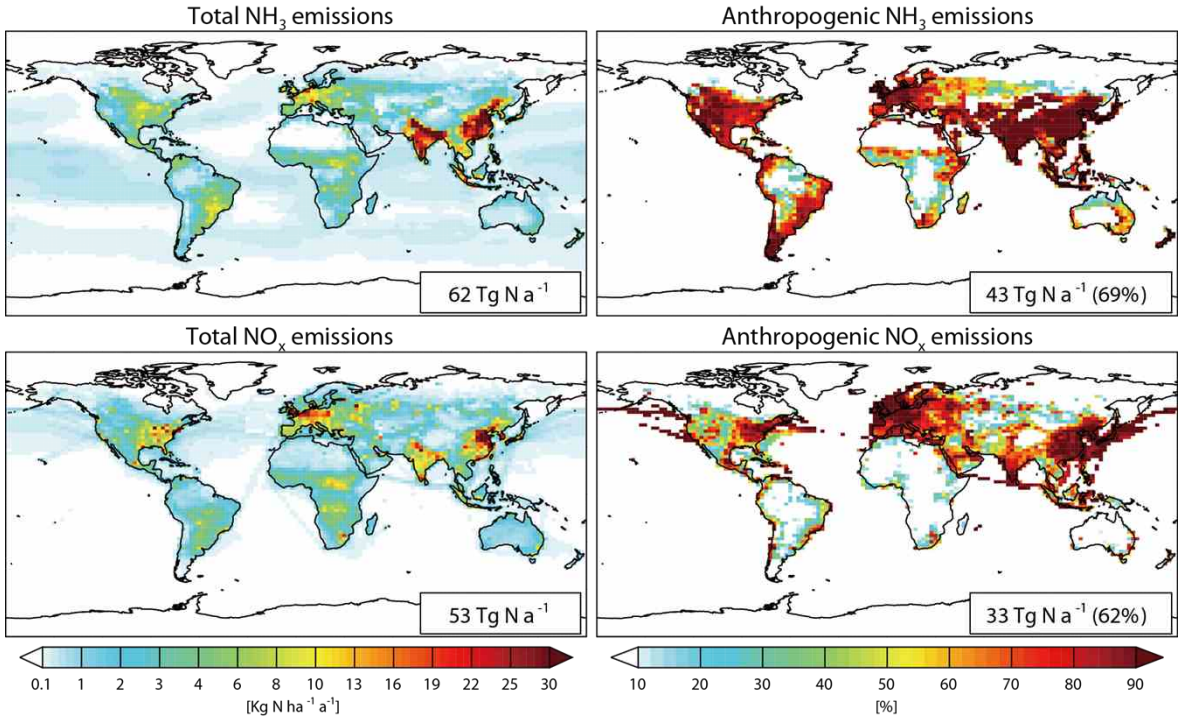

Figure 2. Spatial distribution of total NH_3 (top panels) and NO_x (bottom panels) emissions (left panels) and percentage contribution from anthropogenic sources (right panels) averaged for 2006-2010. Annual global total values are shown inset.

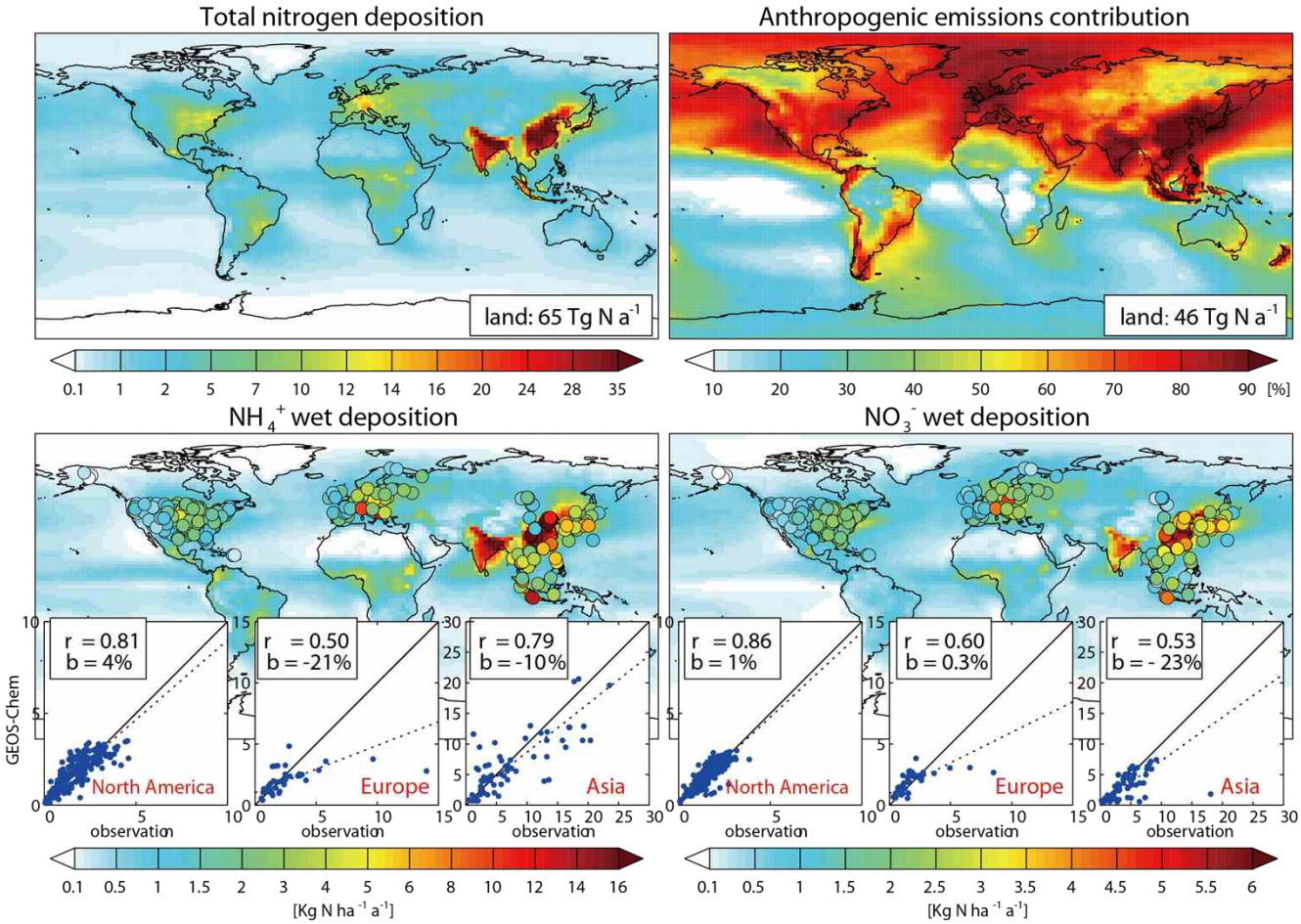

Figure 3. Top panels show total nitrogen deposition fluxes (left) and contributions from anthropogenic sources estimated as percentage changes in the GEOS-Chem simulation with all anthropogenic emissions turned off relative to the simulation with anthropogenic emissions turned on (right). Annual total deposition values to land are shown inset. Bottom panels compare the simulated NH_4^+ (left) and NO_3^- (right) wet deposition fluxes with an ensemble of surface measurements over North America, Europe, and Asia as described in the text. The comparison scatter-plots are over-plotted with correlation coefficients (r) and normalized mean biases (b) also shown inset.

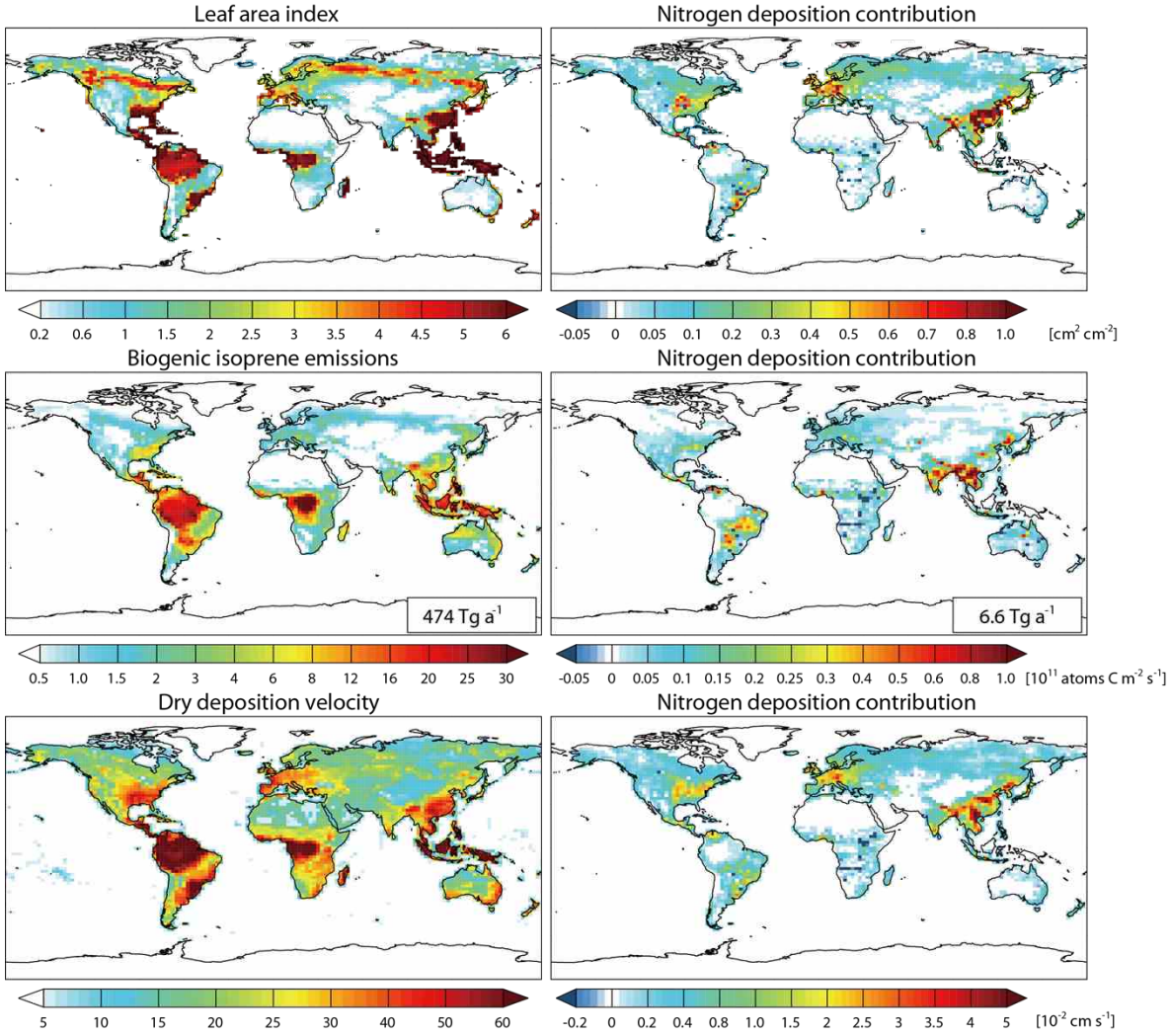

Figure 4. Leaf area index (top panels), biogenic isoprene emission (middle panels with annual total emissions shown inset), and dry deposition velocity for ozone (bottom panels) as simulated by the asynchronously coupled modeling system. The left panels represent the present-day conditions, and the right panels show perturbations as could be driven by human-induced atmospheric nitrogen deposition.

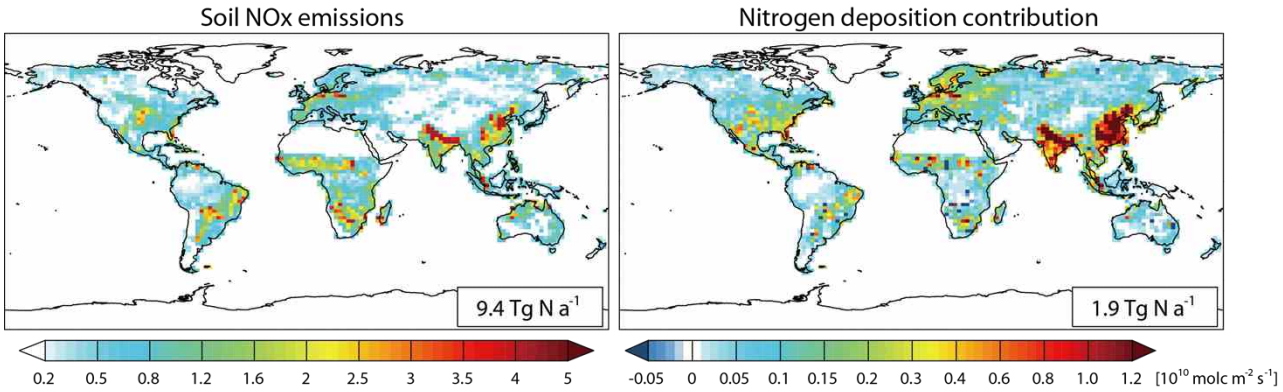

Figure 5. Present-day soil NO_x emissions (left) and contributions from anthropogenic nitrogen deposition (right). Annual totals are shown inset.

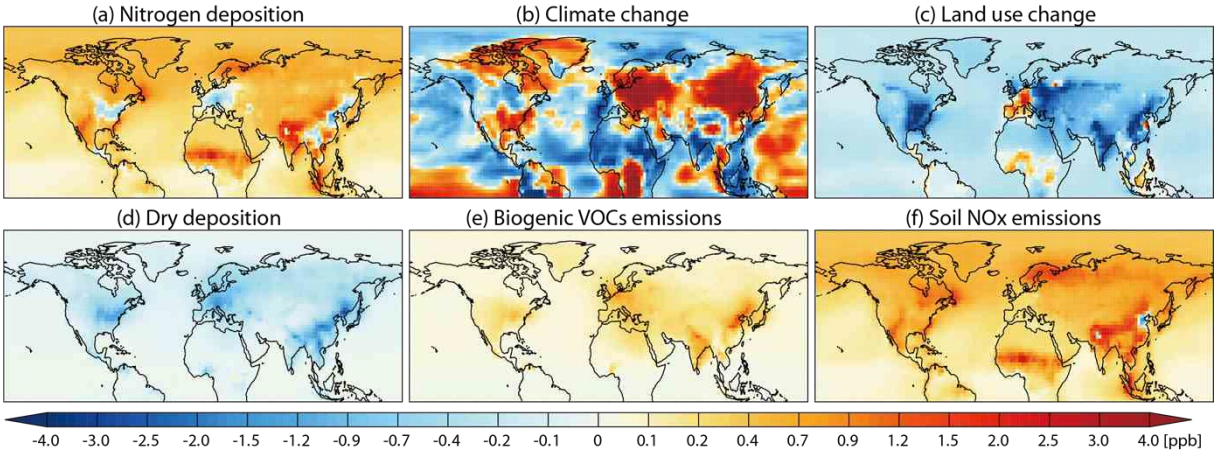

Figure 6. Changes in mean surface ozone concentration for June-July-August driven by anthropogenic nitrogen deposition (top-left panel), changes in climate (2006-2010 vs. 1986-1990; top-middle panel) and land use (present-day vs. 1860 conditions; top-right panel). Model simulations are described in the text. Bottom panels separate the anthropogenic nitrogen deposition-induced ozone changes into those due to three processes: changes in dry deposition velocity, biogenic VOC emissions, and soil NO_x emissions.

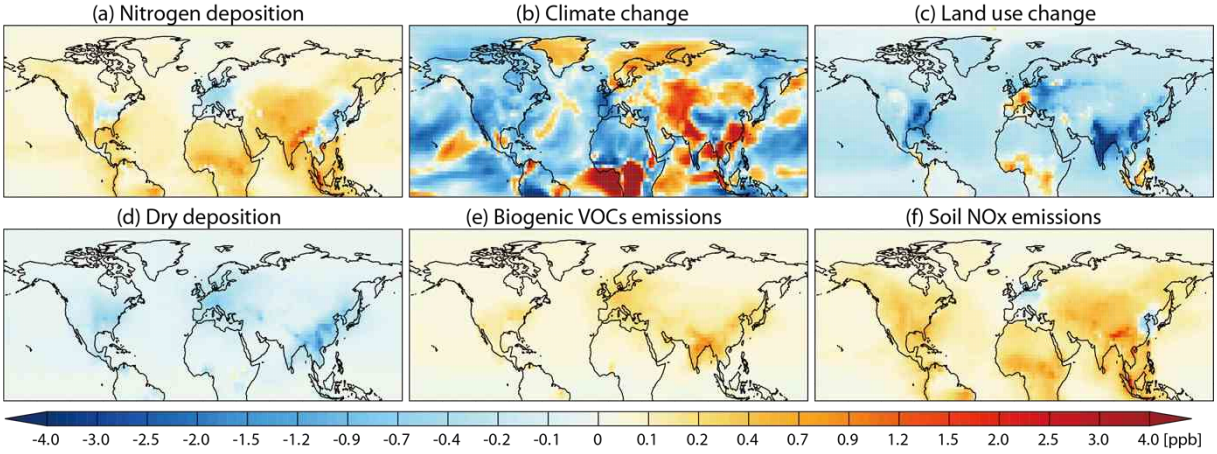

Figure 7. Same as Figure 6 but for March-April-May.